Conductance through a quantum dot in the fractional quantum Hall regime

Jari M. Kinaret, Yigal Meir,* Ned S. Wingreen,† Patrick Lee, and Xiao-Gang Wen

Department of Physics, Massachusetts Institute of Technology, Cambridge, Massachusetts 02139

We study a parabolic quantum dot in the fractional quantum Hall regime by solving the problem exactly for up to eight electrons at filling factors between 1 and $\frac{1}{3}$. Many-body coherence in the fractional regime strongly suppresses the resonant conductance through the dot below the integer-regime values. In particular, we predict that at $\nu = \frac{1}{3}$ all conductance peaks are lowered by a factor of $1/N$, and that at $\nu = \frac{2}{3}$ odd and even peaks are suppressed differently.

Advances in microfabrication techniques have recently made it possible to fabricate electronic devices on the nanometer scale. The physics of electron interactions in these new devices has attracted a great deal of both experimental and theoretical interest. For example, novel resonances have been observed in the conductances of these devices as a function of gate voltage in the presence of a magnetic field.[1] Analysis of the experimental data in view of a recent theory[2,3] yielded detailed information on the single-electron levels in the quantum dot in the integer quantum Hall regime. The situation in the fractional quantum Hall regime is quite different and no theoretical predictions exist for the conductance. In this paper, we solve the problem exactly for up to 8 electrons in a quantum dot in the fractional quantum Hall regime. A similar approach was used earlier[4] to discuss the properties of a quantum dot at filling factor $\nu = \frac{2}{3}$. Our work focuses on the experimentally observable effects of many-electron correlations in a quantum dot in the fractional quantum Hall regime. In particular, we predict that many-body coherence leads to a strong, filling-factor-dependent suppression of the conductance between two electrodes coupled to each other via the dot. The good agreement between our exact wave functions and those based on Laughlin states leads us to believe that these predictions are valid for larger dots as well.

We consider an interacting two-dimensional electron gas, in a magnetic field, confined in the plane by a parabolic potential $\frac{1}{2}m\omega_0^2 r^2$. Throughout this paper we limit our discussion to the regime of sufficiently high magnetic fields perpendicular to the plane such that only the lowest kinetic-energy level is occupied. Since the Hamiltonian H is cylindrically symmetric (in symmetric gauge), it commutes with the angular momentum operator, and its eigenstates can be written as

$$\psi_{M,\alpha} = \exp\left(-\frac{1}{4}\sum|z_i|^2\right) P_{M,\alpha}(z_1, \ldots, z_N) \prod_{\substack{i,j \\ i<j}} (z_i - z_j),$$

$$(1)$$

where $P_{M,\alpha}$ is an Mth order symmetric polynomial of N variables and $z_j = x_j + iy_j$ gives the coordinate (x_j, y_j) of the jth electron. The length scale is chosen so that the effective magnetic length $l_{eff}(B)$—which is given by $l_{eff}^{-2}(B) = m\omega_{eff}/\hbar$, where $\omega_{eff} = (4\omega_0^2 + \omega_c^2)^{1/2}$ and ω_c is the cyclotron frequency—is set equal to unity. It is a special feature of the parabolic potential that the magnetic field only appears in the length scale and does not affect the functional form of the states. The quantum number M denotes the *excess* angular momentum of a state so that the total angular momentum is given by $L = \frac{1}{2}N(N-1) + M$, and α enumerates the different eigenstates with the same M. In the absence of electron-electron interactions, states with the same excess angular momenta are degenerate. This degeneracy is broken by interactions, and the energy is given by

$$E_{N,M,\alpha} = \frac{1}{2}\hbar\omega_{eff}\{[\frac{1}{2}N(N-1) + M](1 - \omega_c/\omega_{eff})$$
$$+ N + \frac{1}{2}N(N-1)\xi_{N,M,\alpha}\}, \qquad (2)$$

where $\xi_{N,M,\alpha}$ is the expectation value of the electron-electron interaction $V(r)$ in the many-body eigenstate $\psi_{M,\alpha}$. Our aim is to find $\psi_{M,\alpha}$, the exact N-electron eigenstates. Since the interaction does not couple many-particle states with different angular momenta, we solve each angular momentum separately in three steps: (a) enumerate all possible N-particle basis states $|NM\beta\rangle$ with a given angular momentum, (b) calculate the interaction matrix $\langle NM\beta'|V|NM\beta\rangle$, and (c) diagonalize the matrix.

To facilitate step (a) we use the fact that the center-of-mass coordinate separates in our problem. In contrast to cyclotron resonance,[5] which couples to the center-of-mass motion,[6] only the lowest-energy states of the dot contribute in a conductance measurement at low temperatures, and center-of-mass excitations can be excluded. In the following we construct states which explicitly exclude the center-of-mass motion. We construct a basis from the primitive symmetric polynomials $\sigma_N^{(h)}$, which are given by sums of all h-term products of N variables, i.e., $\sigma_N^{(1)} = \sum z_i$, $\sigma_N^{(2)} = \sum_{i<j} z_i z_j$, $\sigma_N^{(3)} = \sum_{i<j<k} z_i z_j z_k$, etc. All symmetric polynomials of N variables can be written as sums of products of primitive symmetric polynomials.[7,8] To exclude the center-of-mass component we perform a change of variables and consider σ's of the variables $z_i - \bar{z}$, where $\bar{z}$ is the complex center-of-mass coordinate $\bar{z} = (1/N)\sum z_i$. The products of these polynomials can be used as a basis of symmetric polynomials of order M without center-of-mass motion. The exclusion of center-of-mass degrees of freedom reduces the number of basis states significantly.

The interaction potential is taken to be $V(r) = q^2\hbar^2/2mr^2$, which allows us to evaluate the interaction matrix elements *analytically* [step (b)]. The coupling strength q^2 is only a scale factor in the last term in (2) and has

been set equal to 1 in the subsequent discussion.

In order to interpret our results and make experimental predictions for larger dots we want to describe the exact eigenstates in a way which can be extended to larger systems. Therefore, we first construct an average filling factor $v_{av} = N\Phi_0/2\pi B\langle r^2\rangle = N^2/2(N+L)$. For large N this agrees with the filling factor for Jastrow states $v_J = N(N-1)/2L$. We have solved the eigenstates of systems of 3–8 electrons up to excess angular momentum $M = 18$ corresponding to average filling factors down to $v_{av}^{min} = \frac{3}{16} \approx 0.19$ for $N = 3$ and $v_{av}^{min} = \frac{16}{27} \approx 0.59$ for $N = 8$.

While for large systems the filling factor is constant throughout the bulk, in small systems the edge is much more important and the average filling factor only serves as a guide and does not specify the state uniquely. A more useful way to characterize a few-electron state is via $n(m)$, the occupation of single-particle states of definite angular momenta $m = 0, 1, 2, \ldots$, [4]

$$n(m) = \langle c_m^\dagger c_m \rangle. \tag{3}$$

For the $v = 1$ case $n(m)$ is 1 for $m < N$ and zero otherwise.

In Fig. 1(a), we display the occupations of single-particle states for the lowest-energy eigenstate of 8 electrons with excess angular momentum $M = 14$. At particular filling factors, for large N, it has been suggested that the ground states are given by the particle-hole symmetric counterparts of Laughlin states.[9] Specifically, these N-electron wave functions are described by P holes in the $1/p$ Laughlin state in a background of $N+P$ electrons in the $v = 1$ state. These Laughlin-like states have excess angular momenta

$$M = \frac{1}{2}(N+P)(N+P-1) - (p/2)P(P-1)$$
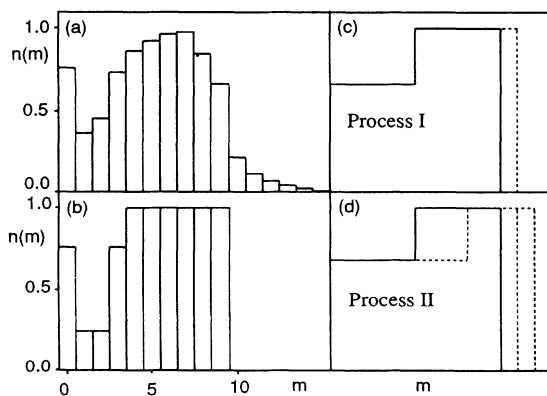$$- \frac{1}{2}N(N-1),$$

FIG. 1. (a) Single-particle occupations in the lowest 8-particle eigenstate with excess angular momentum $M = 14$. (b) Single-particle occupations in the 8-electron particle-hole symmetric state with $P = 2$ and $p = 3$. The overlap between this state and the exact state shown in (a) is 0.75. (c) Schematic picture of the transition at $v = \frac{2}{3}$ from an $(N-1)$-particle state to an N-particle state through process I. Solid line, occupations near the edge of the system of $N-1$ particles; dashed line, occupations near the edge of the system of N particles. (d) Schematic picture of the transition through process II.

and have core filling factors $v = 1 - 1/p$ over the central fraction of the dot, in the large N limit. For example, the state with $N = 8$, $P = 2$, and $p = 3$ has $M = 14$. The single-particle occupations in this state are shown in Fig. 1(b), and the resemblance to $n(m)$ of the exact lowest-energy eigenstate suggests the identification of the latter as the $v = \frac{2}{3}$ particle-hole symmetric state. We find that for those M for which a particle-hole symmetric construction exists, the lowest eigenstate can be identified in this way. The overlap between the exact many-particle state and the corresponding particle-hole symmetric construction varies from 0.6 to 0.8 for those states that could be identified. In Fig. 2 we show the ground states of systems with 3–8 electrons as a function of the magnetic field. All but two of them can be identified using particle-hole symmetry. [For compactness, the notation (P,p) denotes a state with P holes in the $1/p$ state.] The stability of the $v = \frac{2}{3}$ states (shaded in Fig. 2) increases with the number of particles as expected, and we see the appearance of a $v = \frac{4}{5}$ state for $N = 8$. The $v = \frac{1}{3}$ states that we refer to later occur at stronger magnetic fields and do not appear in Fig. 2.

In the *integer* quantum Hall regime it has been possible to experimentally study the conductance through a dot as a function of gate voltage.[1] The dot is weakly coupled to two electrodes and when the chemical potential of the electrodes coincides with the energy difference between the $(N-1)$- and N-particle states of the dot, the conductance of the system exhibits a resonant peak. By studying the movement and relative heights of these peaks as the magnetic field is varied one obtains detailed information about the electronic structure of the dot.

The height and width of a resonant peak for a ground-state–to–ground-state transition are determined by Γ_L and Γ_R, which are given by

$$\Gamma_{L/R} = |\langle NM\alpha|c_{M}^\dagger|(N-1)M'\alpha'\rangle|^2 T_{\Delta L,L/R}. \tag{4}$$

In (4), $T_{m,L/R}$ is the square of the tunneling matrix element to the left-right electrode for angular momentum m, multiplied by the electrode density of states. The first term on the right measures the overlap between the states
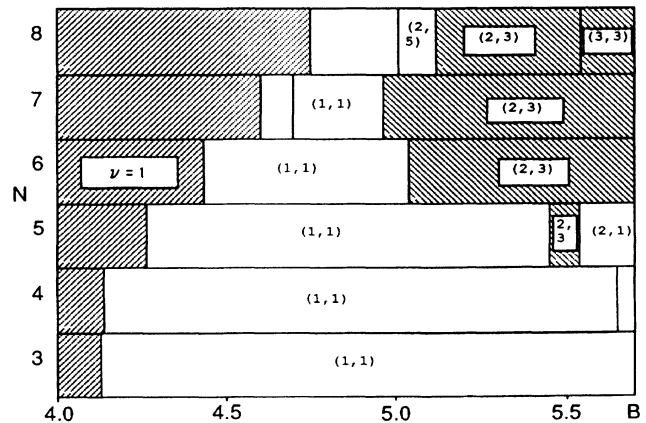

FIG. 2. Ground states of N-electron systems as a function of B in units of $m\omega_0/e$. The shaded regions correspond to $v = 1$ and $\frac{2}{3}$. The notation (P,p) denotes a state with P holes in the $1/p$ state in a background of electrons in the $v = 1$ state.

of $N-1$ electrons, plus one additional electron with the appropriate angular momentum $\Delta L = N - 1 + M - M'$, and the state of N electrons. In the *integer regime* this overlap is *unity* but in the *fractional regime* it can be significantly *less* than 1. At very low temperatures, $kT \ll \Gamma_{L/R}$, the width of a resonant peak is expected to be $(\Gamma_L + \Gamma_R)$, and we expect the overlap factors to reduce the peak widths below the integer regime values. At higher temperatures or weaker couplings, $kT \gg \Gamma_{L/R}$, peak widths are determined by kT, and peak heights are proportional to $\Gamma_L \Gamma_R / (\Gamma_L + \Gamma_R)$—thus we expect the coherence effects to lower the peak height in this regime. In the remainder of this paper we will concentrate on the lattice case.

We first evaluated the overlap matrix element between $v = \frac{1}{3}$ Laughlin states with $N - 1$ and N particles and found that it decreases as $(N - \frac{1}{2})^{-1/2}$ (Fig. 3). We also evaluated the overlap matrix element between the exact lowest-energy eigenstates of H at filling factor $\frac{1}{3}$. The results agree with those obtained for the Laughlin state to within 3.5% and 2.5% for $N = 4$ and 5, respectively.

There is a simple way to understand the above results for $v = \frac{1}{3}$ in the thermodynamic limit. First we notice that the low-energy excitations on the edge of the $v = 1/p$ state move with the same velocity.[10] Thus for large x and t we may assume that the low-energy part of the electron propagator is a function of $x - vt$ and has the form

$$G(x,t) = \langle T(\psi(x,t)\psi^\dagger(0)) \rangle = \frac{\exp(ik_F x - iE_F t)a^{\gamma-1}}{(x - vt)^\gamma},$$

where a is a cutoff length scale $(a \approx l_B)$. In the $1/p$ state the angular momentum of an N-particle state is $L(N) = pN(N-1)/2$, so the addition of one electron increases L by pN, which can be viewed as the angular
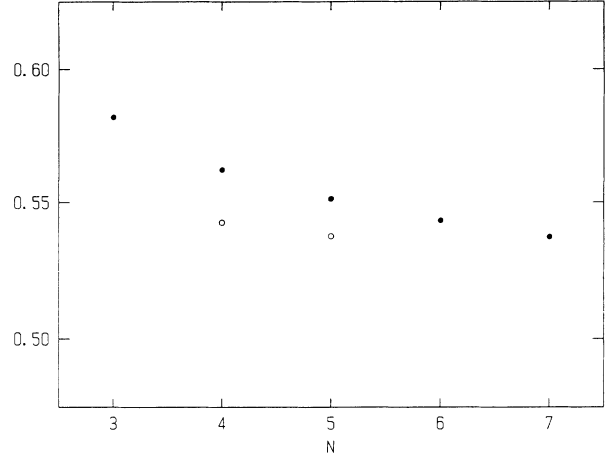

FIG. 3. Overlap matrix elements between $(N-1)$- and N-particle ground states for $v = \frac{1}{3}$, multiplied by $(N - \frac{1}{2})^{1/2}$. Solid dots are for Laughlin states and open dots for the exact eigenstates (zero suppressed).

momentum of the added electron and is denoted by $\tilde{m}(N)$. In the following, we argue that γ is given by $\gamma = \tilde{m}(N) - \tilde{m}(N-1) = p$.

For a quantum dot the electron propagator in the edge obeys periodic boundary conditions and can be written as

$$G(R\theta, t) = \exp(im_F\theta - iE_F t)a^{\gamma-1}R^{-\gamma}(1 - e^{i(\theta - \tilde{v}t)})^{-\gamma},$$

where R is the radius of the dot and $\tilde{v} = v/R$. For $t > 0$ we may expand $G(R\theta, t)$ as

$$G(R\theta, t > 0) = a^{\gamma-1}R^{-\gamma}e^{i(m_F\theta - E_F t)}\left[\sum_{k=0}^{\infty} e^{ik(\theta - \tilde{v}t)}\right]^\gamma. \quad (5)$$

We compare this with the spectral decomposition,

$$G(R, t > 0) = \sum_m \sum_a \langle N|\psi(0)|N+1, m, a\rangle\langle N+1, m, a|\psi^\dagger(0)|N\rangle$$

$$\times \exp\{i[m + L(N+1) - L(N)]\theta\}\exp\{-i[E_{m,a}(N+1) - E_0(N)]t\}, \quad (6)$$

where $|N+1, m, a\rangle$ is an $(N+1)$-electron state with angular momentum $L(N+1) + m$ and energy $E_{m,a}(N+1)$, and $E_0(N)$ is the ground-state energy. The $m = 0$ term contains information about the $(N+1)$-particle ground state, and by comparison with the $k = 0$ term of Eq. (5) we can read off both $m_F = \tilde{m}(N)$ and the overlap matrix element between ground states $|\langle N|c_{\tilde{m}(N)}|N+1\rangle| = (a/R)^{(\gamma-1)/2} \approx N^{-(\gamma-1)/4}$. Finally, γ can be determined by noting that $G(R\theta, t < 0)$ requires a different expansion

$$G(R\theta, t < 0) = (-1)^\gamma a^{\gamma-1}R^{-\gamma}\exp\{i[(m_F - \gamma)\theta - (E_F - \tilde{v}\gamma)t]\}\left[\sum_{k=0}^{\infty} e^{-ik(\theta - \tilde{v}t)}\right]^\gamma. \quad (7)$$

By comparing (7) with a spectral decomposition similar to (6), we find $\tilde{m}(N) - \gamma = L(N) - L(N-1) = 3N - p$, and obtain $\gamma = p$. Furthermore, from the time dependence we find that $E_0(N+1) - E_0(N) = E_0(N) - E_0(N-1) + \tilde{v}\gamma$, i.e., an energy gap exists for the finite-size system. For $v = \frac{1}{3}$ we find $\gamma = 3$ which agrees with the numerical results that suggest the scaling behavior $N^{-1/2}$ for the matrix elements.

Our numerical results for the overlap matrix element in the $v = \frac{2}{3}$ case are shown in Table I. The notation is the same as in Fig. 2, i.e., $(P, p = 3)$ denotes that exact eigenstate of H (not necessarily a ground state) which can be

TABLE I. Overlap matrix elements between $(N-1)$- and N-electron systems for $v = \frac{2}{3}$: (a) $\langle(2,3)|c^\dagger|(2,3)\rangle$, (b) $\langle(3,3)|c^\dagger|(3,3)\rangle$, (c) $\langle(3,3)|c^\dagger|(2,3)\rangle$, (d) $\langle(2,3)|c^\dagger|(3,3)\rangle$. The notation (P, p) denotes a state with P holes in the $1/p$ Laughlin state in the background of $N + P$ electrons in the $v = 1$ state. Columns (a) and (b) correspond to process I in Fig. 1(c), while column (c) corresponds to process II in Fig. 1(d).

N	(a)	(b)	(c)	(d)
6	0.626	$\cdots$	$\cdots$	$\cdots$
7	0.636	$\cdots$	0.344	$\cdots$
8	0.654	0.568	0.248	0.106

identified as a particle-hole symmetric state with P holes in state $\frac{1}{3}$. The empty entries are due to the fact that states with $P=3$ can only be identified for $N=7$ and 8. We see that columns (a) and (b) are close to unity, whereas columns (c) and (d) give smaller overlaps. Column (a) extrapolates to a constant in striking contrast to the $(N-\frac{1}{2})^{-1/2}$ behavior in the $v=\frac{1}{3}$ case. Energetically favorable transitions are either by process I, $|N-1,P,p=3\rangle \rightarrow |N,P,3\rangle$ [columns (a) and (b)], where the electron is added to the outermost edge as shown in Fig. 1(c), or by process II, $|N-1,P,3\rangle \rightarrow |N,P+1,3\rangle$ [column (c)] shown in Fig. 1(d). Column (d) describes an energetically very costly transition in which the $v=\frac{2}{3}$ core shrinks while an electron is added to the system. Process II can be thought of as process I plus a particle-hole excitation whereby an electron is transferred from the inside to the outside edge, thereby expanding the $v=\frac{2}{3}$ region. Because the coupling between the holelike excitations on the inner edge and the electronlike excitations on the outer edge is not known explicitly, we cannot yet make detailed analytical predictions of how the peak heights due to processes I and II scale with N; however, our numerical results suggest that conductance peaks due to process I are higher than those due to process II. In order to preserve the $n(m)$ structure of the edge region, processes I and II must alternate as electrons are added to the dot. Thus in a measurement of conductance versus gate voltage we expect the heights of successive peaks to be different due to the different overlap factors. This doubling of the periodicity with N is expected on the general ground that for $v=\frac{2}{3}$ two added electrons are required to change the flux by an integer amount. This prediction is clearly limited to low temperatures where thermal excitation of process I is suppressed. The I, II ordering of the peaks may also switch as a function of N or the magnetic field as the structure of the edge region evolves, but its detailed description is beyond the scope of the present small-N study.

As the magnetic field is varied at core filling factor $v=\frac{2}{3}$, the height and position of a given conductance peak vary smoothly except at some magnetic field values, when the height changes abruptly. These sudden changes are due to a change of the ground state of either the N- or $(N-1)$-particle system, and the height of a given peak as a function of the magnetic field should exhibit an alternating pattern similar to the alternation of peak heights versus gate voltage. In our numerical study we see one example of this behavior: The peak that corresponds to $7 \leftrightarrow 8$ electrons in the dot is due to process I for $B < 5.53$ and to process II for $B > 5.53$ (Fig. 2), so that the height of the peak is lower by a factor of $(0.248/0.654)^2 = 0.14$ (Table I) for $B > 5.53$. The dependence of the single-particle coupling $T_{m,L/R}$ on angular momentum and geometry may modify this prediction.

In conclusion, we have exactly diagonalized the Hamiltonian describing up to 8 electrons in a parabolic dot in a strong magnetic field. Identifying the exact eigenstates with particle-hole symmetric counterparts of Laughlin states allows us to extrapolate our results to larger, experimentally relevant systems. In particular, we predict that many-body coherence effects will strongly suppress the resonant peaks in a measurement of conductance through a quantum dot in the fractional quantum Hall regime. At the simple filling factors $v=1/p$ both numerical and analytical results suggest that the conductance is suppressed by the factor $N^{-(p-1)/2}$, whereas at composite filling factors a more complicated behavior is expected. Specifically, at $v=\frac{2}{3}$ we predict that odd and even peaks will be suppressed differently (at temperatures smaller than the gap to excitations). Finally, let us point out that our discussion was based on the abrupt edge picture, which was realized in the simulations. In the literature an alternative picture has been proposed for smooth confining potentials,[11] and our results do not apply in that case.

*Present address: Physics Department, University of California, Santa Barbara, CA 93106.

†Present address: NEC Research Institute, 4 Independence Way, Princeton, NJ 08540.

[1]P. L. McEuen *et al.*, Phys. Rev. Lett. **66**, 1926 (1991).

[2]Yigal Meir, Ned S. Wingreen, and Patrick A. Lee, Phys. Rev. Lett. **66**, 3048 (1991).

[3]C. W. J. Beenakker, Phys. Rev. B **44**, 1646 (1991).

[4]M. D. Johnson and A. H. MacDonald, Phys. Rev. Lett. **67**, 2060 (1991).

[5]Ch. Sikorski and U. Merkt, Phys. Rev. Lett. **62**, 2164 (1989).

[6]P. A. Maksym and T. Chakraborty, Phys. Rev. Lett. **65**, 108 (1991).

[7]M. Marcus, *Introduction to Modern Algebra* (Dekker, New York, 1978).

[8]S. A. Trugman and S. Kivelson, Phys. Rev. B **31**, 5280 (1985).

[9]S. M. Girvin, Phys. Rev. B **29**, 6012 (1984).

[10]X. G. Wen, Phys. Rev. B **41**, 12838 (1991).

[11]C. W. J. Beenakker, Phys. Rev. Lett. **64**, 216 (1990).